Radiation doses of yttrium-90 citrate and yttrium-90 EDTMP as determined via analogous yttrium-86 complexes and positron emission tomography

Frank Rösch[1, *], Hans Herzog[2], Cornelius Plag[2], Bernd Neumaier[1], Ulrike Braun[2], Hans-Willhelm Müller-Gärtner[2], Gerhard Stöcklin[1]

[1] Institut für Nuklearchemie, Forschungszentrum Jülich, Jülich, Germany
[2] Institut für Medizin, Forschungszentrum Jülich, Jülich, Germany

Received 6 December 1995 and in revised form 10 April 1996

Abstract. Yttrium-90 is used for palliative therapy for the treatment of skeletal metastases, but because it is a pure β^- emitter, data on the pharmacokinetics and radiation doses to metastases and unaffected organs are lacking. To obtain such data, the present study employed yttrium-86 as a substitute for ^{90}Y, with detection by positron emission tomography (PET). The study compared the properties of two different ^{86}Y complexes – ^{86}Y-citrate and ^{86}Y-ethylene diamine tetramethylene phosphonate (EDTMP) – in ten patients with prostatic cancer who had developed multiple bone metastases (the ten patients being divided into two groups of five). Early dynamics were measured up to 1 h post injection (p.i.) over the liver region, followed by subsequent whole-body PET scans up to 3 days p.i. Absolute uptake data were determined for normal bone, bone metastases, liver and kidney. Radiation doses were calculated according to the MIRD recommendations. Based on the pharmacokinetic measurements of the distribution of the ^{86}Y complexes, it was possible to calculate radiation doses for the bone metastases and the red bone marrow delivered by complexes containing ^{90}Y. In 1 cm^3 of bone metastasis, doses of 26±11 mGy/MBq and 18±2 mGy/MBq were determined per MBq of injected ^{90}Y-citrate and ^{90}Y-EDTMP, respectively. The doses to the bone marrow were 2.5±0.4 mGy/MBq for ^{90}Y-citrate and 1.8±0.6 mGy/MBq for ^{90}Y-EDTMP. ^{86}Y and PET provide quantitative information applicable to the clinical use of ^{90}Y. This method may also be useful for the design of other ^{90}Y radiopharmaceuticals and for planning radiotherapy dosages.

Key words: Yttrium-86 – Yttrium-90 – Positron emission tomography – Bone metastases – Quantitative in vivo radiation dosimetry

Eur J Nucl Med (1996) 23:958–966

Correspondence to: F. Rösch

* *Present address:* Institut für Kernchemie, Johannes Gutenberg-Universität Mainz, D-55099 Mainz, Germany

Introduction

Approximately 80% of patients with prostatic carcinoma develop metastatic bone disease and nearly half of them experience bone pain [1]. Among the modalities for management of bone pain, endoradionuclide therapy (ERT) is a well-established approach. It uses compounds having an affinity for bone that are labelled with beta-emitting radionuclides. For some time, phosphorus-32, strontium-89 and yttrium-90 have been available as ^{32}P-phosphate, ^{89}Sr-chloride and ^{90}Y-citrate [2–4]. Chelates of phosphonates of samarium-153 and rhenium-186, namely, ^{153}Sm-EDTMP (ethylene diamine tetramethylene phosphonate) and ^{186}Re-HEDP (1,1-hydroxyethylidine diphosphonate) are reported to have therapeutically useful biodistributions.

The radiation doses to bone metastases as well as to normal bone and radiosensitive organs such as the bone marrow depend on the activity administered and on the pharmacokinetics of the radiopharmaceutical. The accurate determination of these radiation doses is a critical step in the development of a radiotherapeutical. Usually, measuring the uptake kinetics in individual organs and transferring these time-activity data to the MIRD calculation scheme provides the necessary dosage data. For humans such data are available qualitatively in the case of those β^--emitting radionuclides that simultaneously emit a measurable percentage of low-energy photons. Samarium-153 and rhenium-186 are two examples; their decay generates photons of 103 and 137 keV in abundances of 28% and 9%, respectively. Consequently, some target to non-target accumulation ratios were deduced for ^{153}Sm-EDTMP by means of whole-body gamma camera images. Radiation doses were subsequently derived by Logan et al. [5], Eary et al. [6] and Bayouth et al. [7].

^{90}Y is a pure β^--emitter without any accompanying γ-radiation. It is available in a convenient generator system for no-carrier-added syntheses and is efficiently incorporated into radiopharmaceuticals. Since 1990 more

than 50 papers have described ^{90}Y radiotherapy. There are even new initiatives to magnetically enhance ^{90}Y ERT [8].

To date, the calculations of the human doses of radiation from ^{90}Y radiopharmaceuticals have been indirect, based on one of several empirical approaches:

1. Extrapolating to man pharmacokinetic measurements made on animals ex vivo
2. Calculating from measurements of urinary excretion and blood clearance, based on the assumption that unexcreted radioactivity resides exclusively in skeletal metastases [9, 10]
3. Measuring human uptake kinetics by means of bremsstrahlung registration [11–14]
4. Substituting γ-emitting isotopes such as ^{87}Y or ^{88}Y for ^{90}Y and measuring radioactivity by means of gamma scintigraphy [15]
5. Extrapolating from pharmacokinetic data on indium-111 radiopharmaceuticals for the dosimetric calculations of the chemically similar ^{90}Y radiopharmaceuticals [16–21].

Recently an alternative approach was proposed to use PET to quantitatively assess the pharmacokinetics of ^{90}Y radiopharmaceuticals in humans, using the positron-emitting isotope ^{86}Y ($T_{½}$=14.74 h, 32% β$^+$) [22]. The present paper describes the application of this technique for the determination of uptake kinetics and the individual radiation dose of two ^{90}Y radiopharmaceuticals used in the treatment of disseminated bone metastases, namely, ^{90}Y-citrate and ^{90}Y-EDTMP. Although ^{90}Y-citrate has been available for three decades, data from humans on its biodistribution and radiation doses of individual organs are not available. ^{90}Y-EDTMP is not yet routinely used. It has great potential usefulness, however, since phosphonate ligands such as EDTMP promote the selective uptake of trivalent metallic radionuclides in bone and bone metastases. ^{153}Sm-EDTMP, for instance, is currently under clinical trial in the United States. Sm(III) and Y(III) have very similar co-ordination chemistry and charge-to-radius-ratios that allow substitution for Ca(II) in the hydroxyapatite of bone. Recently, clinical studies were reported on the pharmacokinetics of ^{90}Y-EDTMP in rabbits as well as in humans [23].

Materials and methods

Patients. Ten men with prostatic carcinoma and scintigraphically proven bone metastases were studied. Their ages ranged from 54 to 84 years. The patients had normal haematological parameters. Bone scintigrams with technetium-99m methylene diphosphonate were available for all subjects. None had received either radiotherapy or chemotherapy in the preceding 4 weeks. All had normal kidney and liver function. Prior to the study each patient gave written informed consent. Five patients each were chosen for investigation with ^{86}Y-citrate and ^{86}Y-EDTMP.

Preparation of ^{86}Y compounds. ^{86}Y was produced at the Jülich compact cyclotron CV28 via the (p,n)-reaction on 96.3% enriched $^{86}SrCO_3$ target material; chemical processing led to no-carrier-added and radiochemically pure ^{86}Y(III) [24, 25].

The ^{86}Y-citrate and ^{86}Y-EDTMP complexes were synthesised by adding one drop of ^{86}Y(III) stock solution (10^{-4} *M* HCl) to ligand solutions of the following composition: (a) for citrate 3 ml aqueous solution of 7.5 mg/ml sodium citrate, pH 7.4, overall sodium citrate concentration 0.087 *M*, overall ionic strength 0.17 *M*, and 2 ml saline was added to obtain isotonicity; (b) for EDTMP 2 ml aqueous solution of 21.8–36.5 mg/ml EDTMP adjusted with NaOH to pH 7.5, and 1 ml saline was added to obtain isotonicity. The mixed solutions were sterile filtered and assays of pyrogenicity were performed by standard methods. Radiochemical quality control was performed by paper electrophoresis (Tris acetate, pH 6, as electrolyte) for ^{86}Y-citrate and by paper chromatography on MN 261 paper strips using pyridine/ethanol/water (1:2:4) mixtures, pH 7.4, for ^{86}Y-EDTMP. Radiochemical yields were found to be >98% for both complexes.

Radiopharmaceutical safety. The safety of ^{86}Y-citrate and ^{86}Y-EDTMP was ensured by using a sterile pyrogen-free preparation of the radiopharmaceutical, by monitoring the vital signs of each patient before and up to 1 h post injection (p.i.), by obtaining pre- and post-injection haematological profiles (white cells, red cells, platelet counts) and by pre- and post-injection radiochemical analysis of the compounds (blood, urine).

Radiopharmacokinetic studies. Patients had an intravenous line placed in each arm. Prior to the emission scans total-body transmission scans were recorded. The radiopharmaceuticals were administered intravenously in a volume of 4–5 ml. The administered activities for each subject are listed in Table 3. Dynamic PET scans were started simultaneously with the injection of the radiopharmaceutical and continued for 40–90 min. The field of view covered the liver and/or individual metastases in vertebrae. Later, up to four whole-body PET scans were acquired, the first at about 3 h p.i. and the last up to 76 h p.i.

To determine clearance from the blood, samples of venous blood were withdrawn at 1, 3, 5, 10, 20, 40, 60, 120 and 240 min p.i. The quantity of ^{86}Y excreted in the urine was measured periodically up to 24 h p.i. to obtain the total-body clearance by urinary excretion. Radioactivity in 1-ml aliquots of blood and urine was measured by γ-spectrometry. The activity in the blood pool at each time point was calculated from the measured activity per unit volume in the blood samples and the estimated blood volume [26]. If blood clearance kinetics showed two different phases, the first (fast) and second (slow) phases were denoted with half-lives of $T\alpha_{½}$ and $T\beta_{½}$. Results for $T\alpha_{½}$ refer to the periods from 0 to 5 min and 0 to 4 min p.i. for ^{86}Y-citrate or ^{86}Y-EDTMP, respectively, while those for $T\beta_{½}$ refer to the periods from 60 to 240 min and 20 to 240 min p.i., respectively.

The product of the radioactivity per unit volume of urine multiplied by the volume of that specimen, summed over all specimens, indicated the cumulated clearance of ^{86}Y-citrate or ^{86}Y-EDTMP. The activity in the whole body, $A_{WB}(t)$, was obtained as the difference between whole-body activity and cumulative urinary excretion, $A_U(t)$. This is represented as $A_{WB}(t)=A_O-A_U(t)$, where A_O is the injected activity.

Moreover, blood and urine samples were analysed radiochemically by standard methods. After centrifugation, aliquots of the samples were transferred to a Sephadex G-25 column (20×2 cm). Radioyttrium fractions bound to serum proteins were chromatographically separated from the low-weight radioyttrium complexes using TRIS acetate (0.075 *M*, pH 7) as eluent. Elution profiles were recorded by UV as well as by radioactivity detectors. Indi-

vidual fractions were subsequently collected and the amount of the two fractions was determined in percent.

PET measurement and data analysis. PET measurements were done with the Scanditronix/GE scanner PC4096-15WB [27]. As whole-body transmission scans were recorded before the first PET scan, all emission data could be corrected for attenuation. The patient was very carefully positioned for each measurement by means of laser beams in order to match the position of the transmission scan. The whole-body scans consisted of a series of single scans, each lasting 4–6 min, extending from the neck to the femur. In order to limit the time of investigation, other parts were imaged only if the bone scintigrams showed metastases. Depending on the extent of the whole-body scan, the reconstruction of the emission data yielded up to 210 transverse images for each measurement. These images could be reconstructed as anterior, lateral, coronal or sagittal sections.

The images had the unit ^{86}Y activity concentration, i.e. kBq/cm^3. These primary data were corrected for the β^+-abundance of 32% of ^{86}Y. This accuracy of the activity determination in structures not confounded by the partial volume effect was validated by phantom measurements. The contribution of the few γ-lines of ^{86}Y seen within the energy window of the scanner was satisfyingly corrected. The activity concentration in kBq/cm^3 in the metastases was directly obtained by analysing regions of interest (ROIs) in the transverse slices, using a 30% isocontour level in three adjacent slices, and averaged taking into account the ROI areas. Furthermore, ROIs were marked over normal bone, liver and kidneys. The activity concentration for the liver is given as the mean of at least two different ROIs and that for the kidneys as the mean of one ROI per left and right kidney.

Finally, all data were corrected for the decay of ^{86}Y. Thus, the corrected data served for calculations of the absolute uptake kinetics of the ^{86}Y radiopharmaceuticals. Radionuclide concentrations are expressed in absolute units of kBq/cm^3 and, in some cases, in relative units of %ID/cm^3 or %ID/organ.

Calculation of radiation dose. Calculation of the radiation dose to the metastases, the red marrow, the liver and the kidneys was performed as described in detail elsewhere [22], in accordance with MIRD pamphlets no. 11 and no. 5 [28, 29]. The decay-corrected pharmacokinetic data of the ^{86}Y radiopharmaceuticals were considered to be valid for the analogous ^{90}Y-labelled compounds. A dose constant of 0.54 g·Gy/MBq·h (=2 g·rad/μCi·h) for ^{90}Y and a specific density of bone of 1.5 g/cm^3 were used. The radiation dose to the red marrow was considered to be caused by activity equally stored in cortical and trabecular structures of healthy bone, i.e. the corresponding individual MIRD radiation dose S-factors delivered from ^{90}Y stored in cortical and trabecular bone were applied.

Using the experimental data on excreted urine, the residence time for activity in the bladder content was determined as suggested in example 7 of the MIRD Primer [30] assuming voiding intervals of 2 h and 4 h, respectively.

In order to calculate the cumulated activities for both normal bone and metastases, the activity was considered not to be released after the uptake processes, which are completed at about 40 h p.i. for ^{86}Y-citrate and at about 2 h p.i. for ^{86}Y-EDTMP. This assumption is supported by our measurements over 3 days. This means that the short early periods of uptake can be negelected for the calculation of the cumulated activities. The activities averaged at 48 and 72 h for both ^{86}Y-citrate and ^{86}Y-EDTMP, respectively, were regarded as final levels of $A_{\text{metastasis}}$. With a biological decay constant of zero, the effective half-life equals the physical half-life of ^{90}Y ($T_{1/2}$=64 h), so that the cumulative activity is $\tilde{A}=A_0 \cdot 64\ \text{h} \cdot \ln 2$.

The individual radiation doses are reported as mean ±1 standard deviation. Due to the uncertainty in the parameters comprising the absorbed dose calculations, not more than two significant figures were used in reporting the absorbed dose results.

Results

PET imaging

Figure 1 shows typical transverse images displaying normal spine and bone metastases in a patient injected with ^{86}Y-EDTMP. Figures 2 and 3 compare typical whole-body views (recorded at 22 h p.i.) of ^{86}Y-citrate and ^{86}Y-EDTMP in anterior and midline sagittal projections. Similar results were obtained in the other patients of each group. Both radiopharmaceuticals show the normal skeleton and disseminated bone metastases as hot spots. However, the images produced by the two radiopharmaceuticals differ significantly: there is less soft tissue background in the ^{86}Y-EDTMP images and only the ^{86}Y-citrate images show the liver.

Pharmacokinetics

Early kinetics. Figure 4 shows the early phase of ^{86}Y-citrate uptake (0–60 min p.i.) in patient 4. Initially, a 10-cm-broad body section over the liver was monitored that included some parts of the kidneys as well as a metastasis in the os ilium. Thus, these images served for measurements of the individual uptake kinetics of bone metastases, normal bone and liver and kidneys. ^{86}Y accumulated continuously in bone metastases and also in normal bone, though at a much lower level. ^{86}Y-citrate concentrated in the liver rapidly, reaching a maximum of about 20%ID at 2–3 min p.i. The isotope was then released with a mean half-life of $T_{1/2}$=90±20 min. The kinetics of uptake by and release from the kidneys was similar to that for the liver. Maximum accumulation in the kidneys occurred somewhat later than in the liver, at about 3–5 min p.i. Within the first hour p.i., the release from this organ occurred with a $T_{1/2}$=80±30 min.

Figure 5 shows the early uptake kinetics of ^{86}Y-EDTMP in patient 6. Uptake by bone metastases was faster than that of ^{86}Y-citrate. Absolute values of ^{86}Y activity concentration varied significantly for individual bone metastases. In the kidneys, ^{86}Y uptake reached a maximum at about 2–5 min p.i., followed by a biphasic release consisting of a fast component having a $T\alpha_{1/2}$=15±5 min that lasted for up to 15 min p.i. and a slower component having a $T\beta_{1/2}$=50±10 min evident between 15 and 90 min p.i. Unlike following the injection of ^{86}Y-citrate, the liver showed a much lower accumulation of ^{86}Y-EDTMP.

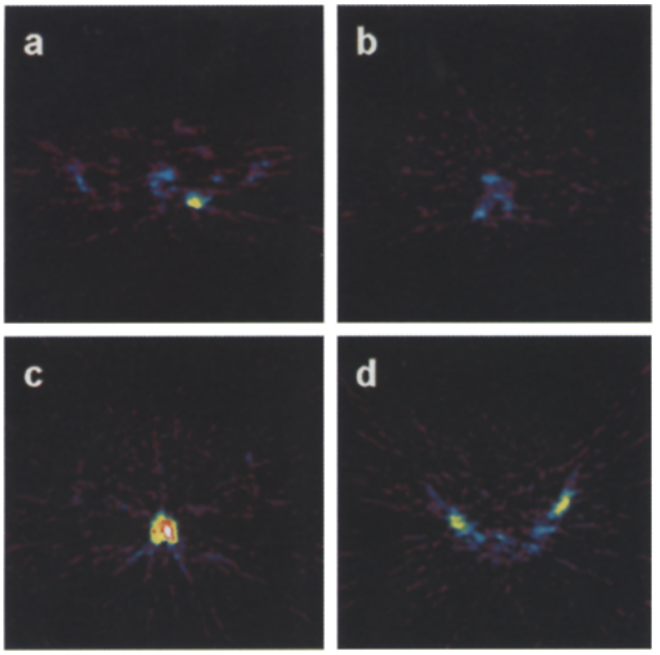

Fig. 1a–d. Transverse images of 6.5-mm thickness recorded 4 h after injection of ^{86}Y-EDTMP in patient 10. Uptake is demonstrated in different bone metastases in the upper thorax (**a**), and in healthy spine (**b**), thoracic spine (**c**) and pelvis (**d**)

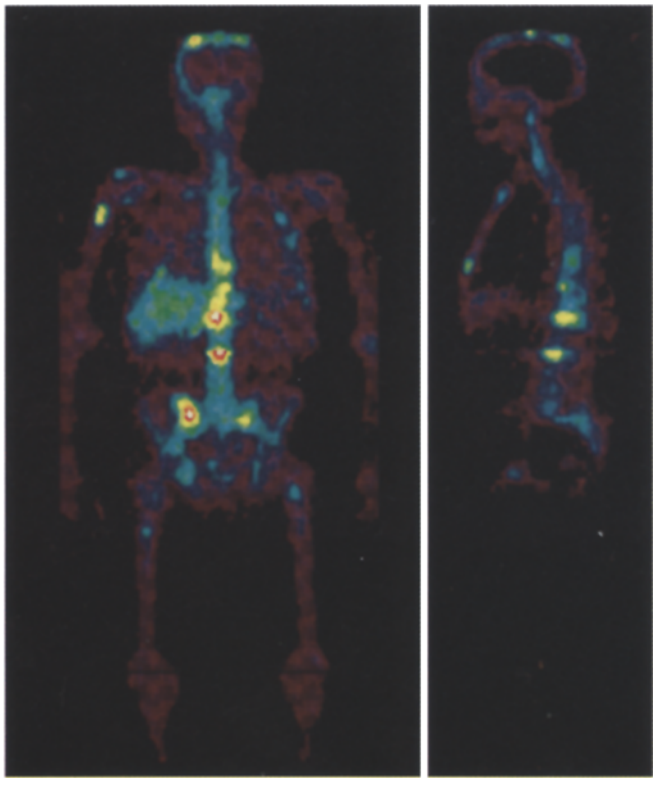

Fig. 2. Whole-body images of the distribution of ^{86}Y-citrate in patient 1 at 22 h p.i. *Left:* Anterior view with all coronal sections summed. *Right:* Sagittal section of 8-cm thickness in the median plane of the patient's body

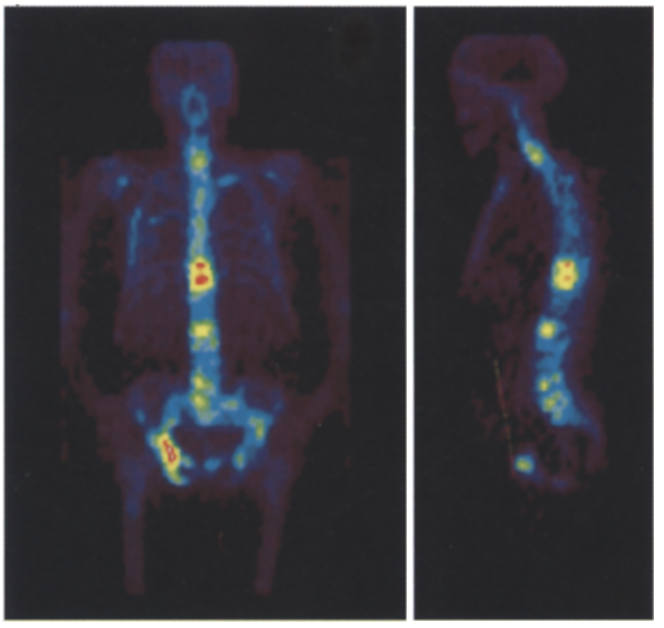

Fig. 3. Whole-body images of the distribution of ^{86}Y-EDTMP in patient 10 at 22 h p.i. See legend to Fig. 2 for further explanation

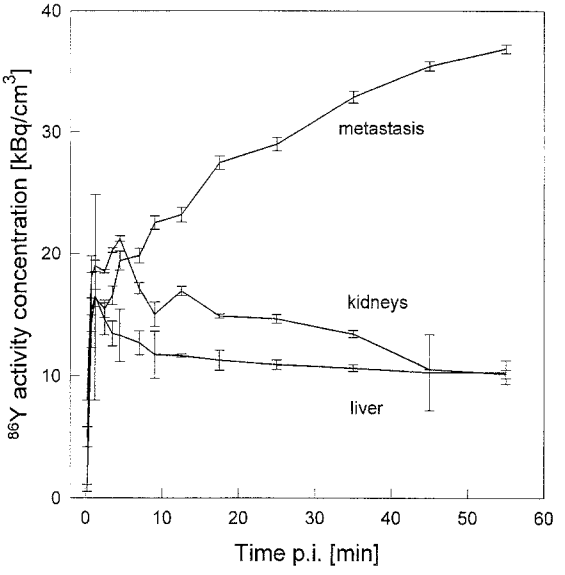

Fig. 4. Decay-corrected initial time-activity curves of the early uptake kinetics of ^{86}Y-citrate in bone metastases, liver and kidneys (patient 4). *Bars* show deviations derived from ROI determinations for an individual metastasis, from two different ROIs for the liver, and from individual ROIs per left and right kidney

Overall kinetics. The overall uptake kinetics covers a period of up to 3 days p.i. Figures 6 and 7 show complete time-activity curves for all the individual bone metastases of patient 4, who received ^{86}Y-citrate, and of patient 6, who received ^{86}Y-EDTMP. The curves for ^{86}Y-EDTMP are typical for all the patients of that group. After correction for decay, the activity concentration in bone metastases was essentially constant as early as ≈1.5 h

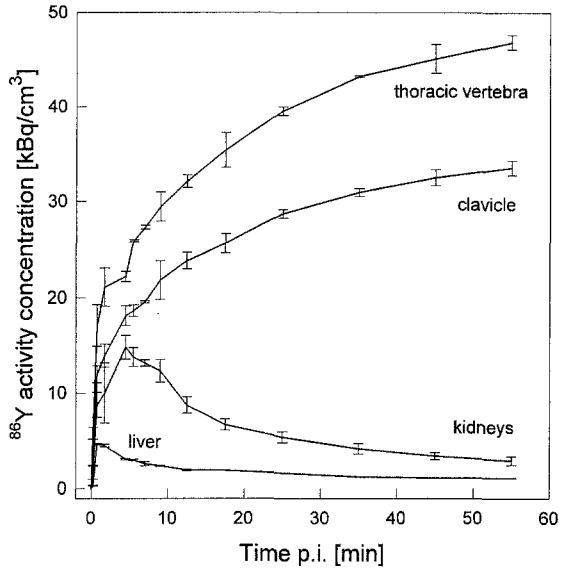

Fig. 5. Decay-corrected initial time-activity curves of the early uptake kinetics of ^{86}Y-EDTMP in bone metastases, liver and kidneys (patient 6). *Bars* show deviations derived from ROI determinations for two individual metastases, from two different ROIs for the liver, and from individual ROIs per left and right kidney

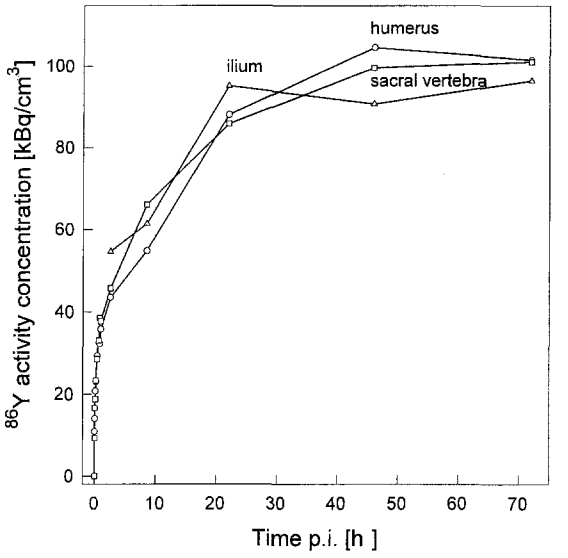

Fig. 6. Complete decay-corrected time-activity curves of various bone metastases, for ^{86}Y-citrate (patient 4)

p.i. In contrast, and also typical for the ^{86}Y-citrate group, activity concentrations in the metastases increased more slowly and reached final levels at approximately 2 days p.i. Average values of the uptake of ^{86}Y-citrate per cm^3 of bone metastases as well as the (total) organ uptake for the skeleton and for the liver are summarised in Table 1. Importantly, the maximum activity concentrations in the ^{86}Y-citrate group were about 50% higher than those in the ^{86}Y-EDTMP group. For both radiopharmaceuticals, once the ^{86}Y activity concentration reached saturation it did not decline, indicating negligible clearance from the metastases.

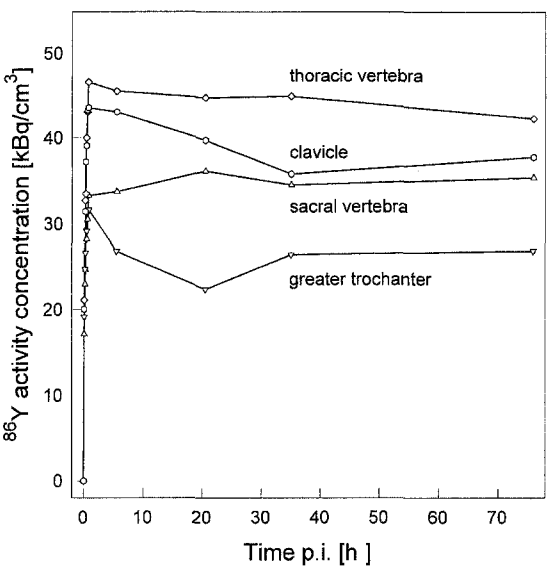

Fig. 7. Complete decay-corrected time-activity curves of various bone metastases, for ^{86}Y-EDTMP (patient 6)

Table 1. Individual uptake of the two ^{86}Y complexes

Radioyttrium complex ligand	Time p.i. (h)	Uptake in various organs (%ID)		
		Bone metastases (per cm^3)	Skeleton (total)	Liver (total)
Citrate	4	0.050±0.018	25.8±4.5	13.6±2.0
	20	0.071±0.028	34.2±5.7	13.9±2.0
	48	0.085±0.037	36.2±5.9	11.2±1.8
	72	0.102±0.013	44.0±1.4	10.0±2.2
EDTMP	4	0.051±0.004	23.5±8.0	[a]
	20	0.050±0.004	24.2±7.7	[a]
	48	0.054±0.008	23.5±7.8	[a]
	72	0.053±0.003	23.8±2.7	[a]

[a] At the background level

Although the kinetics of uptake were similar within each group, the maximum ^{86}Y activity concentrations, expressed as %ID/cm^3, varied not only between patients but also between metastases in the same patient (cf. Fig. 7 for example). Average values of the uptake of both the ^{86}Y-complexes are summarised in Table 1.

The different uptake kinetics of ^{86}Y-citrate and ^{86}Y-EDTMP by bone metastases in turn determine the ratio of ^{86}Y activity concentration ratios between bone metastases and normal bone. In a given patient these ratios varied significantly, from 3:1 to 15:1. Similar ratios of 8±2 were obtained at about 1 h p.i. for ^{86}Y-EDTMP and at about 2 days p.i. for ^{86}Y-citrate. There is evidence that the ^{86}Y uptake kinetics in normal bone is somewhat faster than in bone metastases. The healthy bone seems to be more rapidly covered by ^{86}Y to a final level. The bone metastases may increasingly incorporate ^{86}Y due to the weaker apatite matrix.

Table 2. Blood clearance and urinary whole-body retention data

^{86}Y complex	Patient no.	Ligand concentration	Blood clearance					Whole-body retention
			$T\alpha_{1/2}$ (min)	%ID 10 min p.i.	Time for 50% clearance (min)	%ID 2 h p.i.	$T\beta_{1/2}$ (min)	4 h p.i. (cumulated)
Citrate[a]	3	Isotonic	1.9	16.7	1.5	1.1	90	91
	4	Isotonic	6.3	51.6	11.8	5.9	105	84
	5	Isotonic	4.3	33.3	4.5	2.1	99	98
	Mean		4.2±1.8	34±14	5.9±3.1	3.0±2.1	98±6	91±6
EDTMP	6	43.5 mg	2.1	11.3	1.1	0.7	65	93
	7	75.0 mg	1.3	6.5	1.0	0.3	61	(18)
	8	45.6 mg	2.2	25.4	1.5	1.3	59	65
	9	48.9 mg	6.5	43.3	7.6	4.7	150	72
	10	46.0 mg	2.1	19.0	1.1	3.5	70	64
	Mean		2.8±0.9	21±6	2.5±1.3	2.1±0.9	81±38	73±13[b]

[a] Blood pool and urinary excretion was not measured in patients 1 and 2

[b] Calculated without patient 7 because of the higher EDTMP concentration injected

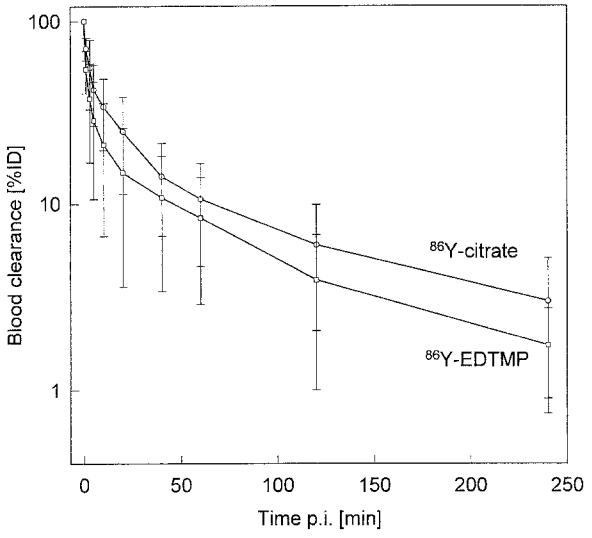

Fig. 8. Average blood clearance kinetics of ^{86}Y-citrate and ^{86}Y-EDTMP. *Bars* show standard deviations (n=3 for ^{86}Y-citrate, n=5 for ^{86}Y-EDTMP)

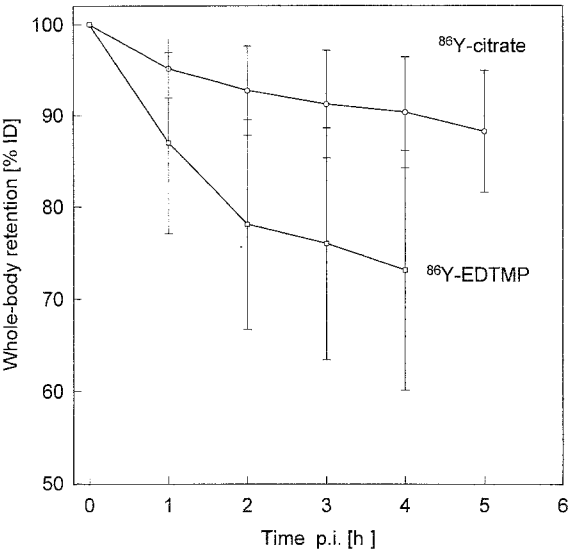

Fig. 9. Average whole-body retention kinetics of ^{86}Y-citrate and ^{86}Y-EDTMP. *Bars* show standard deviations (n=3 for ^{86}Y-citrate, n=4 for ^{86}Y-EDTMP)

For ^{86}Y-citrate, the ^{86}Y activity concentration in the liver peaked at 2–3 min p.i. and then decreased continuously over the whole period of measurement. At 20 h p.i. and 72 h p.i. this organ contained about 14% and 10%, respectively, of the total administered activity (Table 1).

Blood clearance and whole-body retention

Table 2 summarises individual blood clearance and whole-body retention data. Average blood clearance and average whole-body retention kinetics are summarised in Figs. 8 and 9. The clearance of ^{86}Y from blood was biphasic, consisting of a rapid phase lasting about 10 min p.i., followed by clearance at a slower rate (Table 2). An average of 34%±14% of the injected ^{86}Y activity remained in the blood at 10 min after the injection of ^{86}Y-citrate, compared with only 21%±6% of the ^{86}Y-EDTMP activity. The half-times of the rapid clearance phases were $T\alpha_{1/2}$=4.2±1.8 min for ^{86}Y-citrate and 2.8±0.9 min for ^{86}Y-EDTMP. Table 2 also includes the time when 50% of the radioactivity was removed from the blood. At the end of 1 and 2 h, blood radioactivity had dropped to 11%±6% and 3.0%±2.1% for ^{86}Y-citrate and to 7.4%±3.9% and 2.1%±0.9% for ^{86}Y-EDTMP, the values of $T\beta_{1/2}$ for this slow phase being 98±6 min and 64±4 min, respectively.

The whole-body retention of ^{86}Y-citrate by individual patients was very similar, 91%±6% at 4 h p.i. For ^{86}Y-EDTMP the whole-body retention was 73%±13% at 4 h p.i. with one exception. Interestingly, patient 7, who received the highest EDTMP dose of 75 mg, excreted 82%

Table 3. Individual radiation doses calculated for the injection of 1 MBq of the two ^{90}Y complexes

Radioyttrium complex ligand	Patient no.	^{86}Y activity injected (MBq)	Radiation dose (per MBq ^{90}Y injected)		
			Bone metastases[a, c] (mGy/MBq)	Red marrow[b, d] (mGy/MBq)	Liver[d] (mGy/MBq)
Citrate	1	225	22±8	2.0	1.8
	2	130	25±7	3.0	1.6
	3	295	35±1	2.5	
	4	265	36±3	2.9	2.1
	5	180	10±1	2.3	
	Mean		26±11	2.5±0.4	1.8±0.3
EDTMP	6	245	20±5	1.5	
	7	220	16±2	1.9	
	8	150	17±2	1.5	
	9	150	19±6	1.2	
	10	195	17±3	2.7	
	Mean		18±2	1.8±0.6	

[a] Data could not be compared by *t* test. A rank sum test showed no significant difference
[b] A *t* test revealed a significant difference ($P<0.05$) between ^{86}Y-citrate and ^{86}Y-EDTMP
[c] Radiation dose per one cm^3 volume
[d] Radiation dose per organ

ID by 4 h p.i., i.e. the whole-body retention was only 18%.

Biochemical analysis

Radiochemical analysis of blood samples showed that the stability of the two ^{86}Y radiopharmaceuticals differed in vivo. Gel chromatography revealed that 5 min after the injection of ^{86}Y-citrate, >60% of the ^{86}Y in the blood was bound to serum proteins. In contrast, the ^{86}Y-EDTMP complex was much more stable; at 5 min p.i., ^{86}Y bound to serum proteins accounted for only 7% of the blood ^{86}Y activity.

Radiation doses of ^{90}Y radiopharmaceuticals

Using the uptake kinetics measured with ^{86}Y, the radiation dose was calculated for the ^{90}Y analogues, cf. [22]. The individual patient data for the bone metastases, the liver and the red marrow are summarised in Table 3, which also includes mean values and standard deviations of the radiation doses for each radiopharmaceutical.

The average dose to 1 cm^3 of bony metastases, per MBq ^{90}Y injected, would be greater for ^{90}Y-citrate (26±11 mGy/MBq) than for ^{90}Y-EDTMP (18±2 mGy/MBq) ($P>0.05$). ^{90}Y-citrate also would deliver a higher dose to red marrow (2.5±0.4 mGy/MBq) than ^{90}Y-EDTMP (1.8±0.6 mGy/MBq) ($P<0.05$) (Table 3). Due to the negligible uptake of ^{90}Y-EDTMP by liver, only the uptake of ^{90}Y-citrate is relevant, this would be 1.8±0.3 mGy/MBq.

Radiation doses to the kidneys were available for those patients in whom uptake kinetics of the two ^{86}Y-complexes for this organ were measured within the early period of accumulation. For ^{86}Y-citrate, this was the case for patients 3, 4 and 5. According to the varying blood clearance kinetics (cf. Table 2), the residence times for these patients were different too. The calculated data were 4.11 min, 1.74 min and 0.62 min, respectively. This resulted in radiation doses of 0.12, 0.05 and 0.02 mGy/MBq, respectively, per MBq ^{90}Y-citrate injected. In the case of ^{86}Y-EDTMP one patient (no. 9) was analysed. The residence time determined was 1.37 min and the corresponding radiation dose amounted to 0.04 mGy/MBq for ^{90}Y-EDTMP.

Radiation doses to the bladder wall were calculated for patients 3–5 (^{86}Y-citrate) and patients 6–10 (^{86}Y-EDTMP). As these data were derived from the mean values of whole-body retention, cf. Table 2 and Fig. 9, average radiation doses were obtained for this organ in the case of both of the ^{90}Y complexes. Assuming voiding intervals of 2 h and 4 h, the radiation doses were 1.1 and 2.2 mGy per MBq of ^{90}Y-citrate injected, respectively, and 0.9 and 2.1 mGy per MBq of ^{90}Y-EDTMP injected.

Discussion

As expected, both the ^{86}Y radiopharmaceuticals localised primarily in the skeleton. Metastases accumulated ^{86}Y-EDTMP rapidly, attaining maximum concentrations by 1.5 h p.i. ^{86}Y-citrate accumulated much more slowly, requiring about 2 days to reach a maximum, but the level attained was higher than that achieved by ^{86}Y-EDTMP. Once deposited, the ^{86}Y of both radiopharmaceuticals remained in bone metastases or normal bone.

The individual bone metastases to normal bone accumulation ratios for ^{86}Y-citrate and ^{86}Y-EDTMP were similar, ranging between 3:1 and 15:1. However, final average ratios of 8±2 for ^{86}Y-EDTMP were already

reached at about 1 h p.i. and remained constant over the entire period of measurement. For ^{86}Y-citrate, on the other hand, the average ratio at about 1 h p.i. amounted to 6.5±1.5 and increased to 8±2 at 2 days p.i.

Data on the accumulation of ^{86}Y permitted calculation of the radiation doses that would be delivered by ^{90}Y radiopharmaceuticals. Such calculations indicate that ^{90}Y-citrate will deliver a slightly higher dose to 1 cm^3 of metastases than ^{90}Y-EDTMP (26±11 vs 18±2 mGy/MBq ^{90}Y administered, respectively). The ROI technique of evaluating the activity uptake into a single metastasis is influenced by the partial volume effect. Therefore, it is expected that the activity in some parts of the metastasis as well as the related radiation dose will be higher than the data derived from the ROI mean.

The corresponding doses to total bone marrow per MBq administered ^{90}Y, as derived from the accumulation of ^{90}Y in healthy bone, will be 2.5±0.4 and 1.8±0.6 mGy/MBq. Owing to preferential deposition of the radiopharmaceuticals in bone metastases, the local dose to bone marrow in the vicinity of a metastasis could be up to 15-fold higher. This, in turn, will increase the average radiation dose to the bone marrow.

The stabilities of the Y-citrate and Y-EDTMP complexes significantly influence their distributions in the body, their rates of accumulation in bony metastases and, finally, the radiation doses delivered to such metastases. Y-EDTMP is more stable than Y-citrate, the igβ of the complexes being ≈20 and 7.9, respectively [31–33]. Owing to the greater stability of the Y-EDTMP complex, the binding of yttrium to blood proteins and uptake by the liver are negligible, and a greater fraction of the injected dose is immediately available for uptake by bone and bony metastases. The remainder of the $^{86/90}$Y is rapidly excreted via the kidneys.

Some parts of the Y^{3+} released by the dissociation of the citrate complex bind to serum and are taken up by the liver. The sequestration and subsequent slow release of yttrium from these depots accounts for the slow accumulation of the radionuclide in bone and for the greater whole-body radiation dose. On the other hand, it prevents a significant portion of $^{86/90}$Y from being excreted rapidly. This is reflected in the whole-body retention of the two $^{86/90}$Y complexes. In turn, this intermediate storage allows for redistribution of $^{86/90}$Y, providing a steady transfer of the radionuclide from the liver to bone metastases. Consequently, this process is an explanation for the higher activity concentration of ^{86}Y in the bone metastases obtained in the case of ^{86}Y-citrate. The results of the studies of ^{86}Y binding to serum proteins in the present study, as well as studies of the biodistribution of complexes of ^{87}Y(III) with citrate and EDTMP in rats [34], support this interpretation. The replacement of Ca(II) in the hydroxyapatite lattice by Y(III) in the form of Y^{3+} cation is an important mechanism for the deposition of yttrium in bone. For $^{86/90}$Y-EDTMP the binding of the phosphonate moiety to the hydroxyapatite matrix is also important [35]. In both of these processes, the stability of the Y-EDTMP complex would tend to limit the amount of yttrium incorporated and thus could contribute to the lower radiation dose delivered by this radiopharmaceutical.

Conclusion

The clinical application of the β^--emitter ^{90}Y in endoradiotherapy requires quantitative data on both the biodistribution and the radiation dose of ^{90}Y radiopharmaceuticals. Studies employing β^+-emitting ^{86}Y as a substitute for β^--emitting ^{90}Y and direct in vivo measurement by PET compared the pharmacokinetics and radiation dosages of $^{86/90}$Y-citrate and $^{86/90}$Y-EDTMP complexes, each in groups of five patients with bone metastases from carcinoma of the prostate. Owing to the stability of the $^{86/90}$Y-EDTMP complex, sequestration of $^{86/90}$Y in blood and liver was negligible, and concentrations of $^{86/90}$Y in bone metastases reached a maximum by 1.5 h. Because a substantial fraction of the $^{86/90}$Y delivered by the citrate complex is taken up by and then slowly released from the liver, concentrations in metastases required about 2 days to reach a maximum in the case of $^{86/90}$Y-citrate but bone metastasis levels were higher than those achieved with $^{86/90}$Y-EDTMP.

The results of the present study suggest that this technique could be superior to the other methods used to estimate in vivo radiation doses of ^{90}Y radiopharmaceuticals. Moreover, the study demonstrates the feasibility of using this technique to compare different ^{90}Y radiopharmaceuticals in vivo.

Finally, a preliminary ^{86}Y PET trial in an individual patient can serve as a precise basis for calculating the dose of ^{90}Y to be used subsequently in radiotherapy. In determining the activity of ^{90}Y-citrate and ^{90}Y-EDTMP that can be safely administered to a patient, the radiation dose to both bone metastases and the red marrow should be taken into consideration.

Acknowledgements. This work was supported in part by grant Ro 985/2-1 of the Deutsche Forschungsgemeinschaft. We thank the team of the CV28 cyclotron for the irradiations and L. Theelen for technical assistance.

References

1. Campa JA III, Payne R. The management of intractable bone pain: a clinican's perspective. *Semin Nucl Med* 1992; 22: 3–10.
2. Silberstein EB, Elgazzar AH, Kapilivsky A. Phosphorus-32 radiopharmaceuticals for the treatment of painful osseous metastases. Sem Nucl Med 1992; 22: 17–27.
3. Lewington VJ. Targeted radionuclide therapy for bone metastases. *Eur J Nucl Med* 1993; 20: 66–74.
4. Kutzner J, Hahn K, Grimm W, Rösler HP, Eckmann A, Bender S. ^{90}Yttrium-citrate for pain-therapy by bone metastases. *NUC Compact* 1990; 21: 128–132.

5. Logan KW, Volkert WA, Holmes RA. Radiation dose calculations in persons receiving injection of samarium-153 EDTMP. *J Nucl Med* 1987; 28: 505–509.
6. Eary JF, Collins C, Stabin M, Vernon C, Petersdorf S, Baker M, Hartnett S, Ferency S, Addison SJ, Appelbaum F, Gordon EE. Samarium-153-EDTMP biodistribution and dosimetry estimation. *J Nucl Med* 1993; 34: 1031–1036.
7. Bayouth JE, Macey DJ, Kasi LP, Fosella FV. Dosimetry and toxicity of samarium-153-EDTMP administered for bone pain due to skeletal metastases. *J Nucl Med* 1994; 35: 63–69.
8. Raylman RR, Wahl RL. Magnetically enhanced radionuclide therapy. *J Nucl Med* 1994; 35: 157–163.
9. Stewart JSW, Hird V, Snook D, Sullivan M, Myers MJ, Epenetos AA. Intraperitoneal ^{131}I- and ^{90}Y-labeled monoclonal antibodies for ovarian cancer: pharmacokinetics and normal tissue dosimetry. *Int J Cancer* 1988; 3: 71s–76s.
10. Stewart JSW, Snook D, Dhokia B, Sivolapenko G, Hooker G, Taylor Papadimitriou J, Rowlinson G, Sullivan M, Lambert HE, Coulter C, Mason WP, Soutter WP, Epenetos AA. Intraperitoneal yttrium-90-labeled monoclonal antibody in ovarian cancer. *J Clin Oncol* 1990; 8: 1941–1950.
11. Dunscombe PB, Bhattacharyya AK, Dale RG. Technical note. The assessment of the body distribution of yttrium-90 ferric hydroxide during radiation synovectomy. *Br J Radiol* 1976; 49: 372–373.
12. Smith T, Crawley JCW, Shawe DJ, Gumpel JM. SPECT using bremsstrahlung to quantify ^{90}Y uptake in Baker's cysts: its application in radiation synovectomy of the knee. *Eur J Nucl Med* 1988; 14: 498–503.
13. Smith T, Shawe DJ, Crawley JCW, Gumpel JM. Use of single photon emission computed tomography (SPECT) to study the distribution of ^{90}Y in patients with Baker's cysts and persistent synovitis of the knee. *Ann Rheum Dis* 1988; 47: 553–558.
14. Mullan BP, Surveyor I. Imaging yttrium-90 synovectomy studies. *Australas Radiol* 1989; 33: 379–381.
15. Kutzner J, Hahn K, Beyer GJ, Grimm W, Bockisch A, Rösler HP. Scintigraphic use of Y-87 during Y-90 therapy of bone metastases. *Nucl Med* 1992; 31: 53–56.
16. Order SE, Klein JL, Leichner PK, Frincke J, Lollo C, Carlo DJ. ^{90}Yttrium anti-ferritin – a new therapeutic radiolabeled antibody. *Int J Radiat Oncol Biol Phys* 1986; 12: 277–281.
17. Order SE, Vriesendrop HM, Klein JL, Leichner PK. A phase I study of ^{90}yttrium antiferritin: dose escalation and tumor dose. *Antibody Immunoconj Radiopharm* 1988; 1: 163–168.
18. Leichner PK, Nai-Chen Yang, Frankel TL, Loudenslager DM, Hawkins WG, Klein JL, Order SE. Dosimetry and treatment planing for ^{90}Y-labeled antiferritin in heaptoma. *Int J Radiat Oncol Biol Phys* 1988; 14: 1033–1042.
19. Williams LE, Beatty BG, Beatty JD, Wong JYC, Paxton RJ, Shivley JE. Estimation of monoclonal antibody associated ^{90}Y activity needed to achieve certain tumor radiation doses in colorectal cancer patients. *Cancer Res* 1990; 50:1029s–1030s.
20. Vriesendrop HM, Herpst JM, Germack MA, Klein JL, Leichner PK, Loudenslager DM, Order SE. Phase I–II studies of yttrium-labeled antiferritin treatment for endstage Hodgkin's disease, including Radiation Therapy Oncology Group 87-01. *J Clin Oncol* 1991; 9: 918–928.
21. Zimmer AM, Kuzel TM, Spies WG, Duba RB, Webber DI, Kazikiewicz JM, Radosevich JA, LoCicero J, Robinson PG, Gilyon KA, Samuelson E, Spies SM, Rosen ST, Maguire RT. Comparative pharmacokinetics of In-111 and Y-90 B72.3 in patients following single dose intravenous administration. *Antibody Immunoconj Radiopharm* 1992; 5: 285–294.
22. Herzog H, Rösch F, Stöcklin G, Lueders C, Qaim SM, Feinendegen LE. Measurement of pharmacokinetics of yttrium-86 radiopharmaceuticals with PET and radiation dose calculation of analogous yttrium-90 radiotherapeutics. *J Nucl Med* 1993; 34: 2222–2226.
23. Yang Z, Zhang MY, Lin BH, Jin XH. Study of the pharmacokinetics of Y-90-EDTMP. Abstracts of the 6th world congress of the World Federation of Nuclear Medicine and Biology, 23–28 October 1994, Sydney, Australia. *Eur J Nucl Med* 1994; s21; S 126.
24. Rösch F, Qaim SM, Stöcklin G. Nuclear data relevant to the production of the positron emitting radioisotope ^{86}Y via the ^{86}Sr(p,n)- and ^{nat}Rb(^{3}He,2n)-processes. *Radiochim Acta* 1993; 61: 1–8.
25. Rösch F, Qaim SM, Stöcklin G. Production of the positron emitting radioisotope ^{86}Y for nuclear medical application. *Appl Radiat Isot* 1993; 44: 677–681.
26. Nadler SB, Hidalgo JU, Bloch T. Prediction of blood volume in normal human adults. *Surgery* 1962; 52: 22–29.
27. Rota Kops E, Herzog H, Schmid A, Holte S, Feinendegen LE. Performance characteristics of an eight-ring whole-body PET scanner. *J Assist Comput Tomogr* 1990; 14: 437–445.
28. Snyder WS, Ford MR, Warner GG, Watson SB. "S" absorbed dose per unit cumulated activity for selected radionuclides and organs. MIRD pamphlet no 11. New York: The Society of Nuclear Medicine, 1975.
29. Snyder WS, Ford MR, Warner GG, Fisher LH Jr. Estimates of absorbed fractions for monoenergetic photon sources uniformly distributed in various organs of heterogeneous phantom. MIRD pamphlet no 5. *J Nucl Med* 1969; 10: 5s–52s.
30. Loevinger R, Budinger TF, Watson EE. *MIRD Primer*. New York: The Society of Nuclear Medicine; 1988: 31–33.
31. Martell AE. Critical stability constants. Library of Congress cataloging in publication data. New York: Plenum Press, 1989.
32. Tikhonova LI. Investigation of the complex formation of certain alkaline-earth and rare-earth elements with ethylenediamine-*N,N,N′,N′*-tetramethylene-phosphonic acid. (russ.) *Radiokhimiya* 1970; 12: 519–521.
33. Kabachnik I, Dyatlova NM, Medved TT, Begulin YF, Sidolenko VV. Complex formation properties of ethylenediamine-*N,N,N′,N′*-tetramethylene-phosphonic and diethylenetriamine-*N,N,N′,N″,N″*-pentamethylene phosphonic acids. (russ.) *Dokl Akad Nauk* 1967; 175: 351–360.
34. Beyer GJ, Bergmann R, Kampf G, Mäding P, Rösch F. Simultaneous study of the biodistribution of radio-yttrium complexed with EDTMP and citrate ligands in tumour-bearing mice. *Nucl Med Biol* 1992; 19: 201–203.
35. Goeckeler WF, Edwards B, Volkert WA, Holems RA, Simon J, Wilson D. Skeletal localization of samarium-153 chelates: potential therapeutic bone agents. *J Nucl Med* 1987; 28: 495–504.